Journal of Molecular and Cellular Cardiology 85 (2015) 58–70

Contents lists available at ScienceDirect

Journal of Molecular and Cellular Cardiology

journal homepage: www.elsevier.com/locate/yjmcc

Original article

Macrophages and galectin 3 play critical roles in CVB3-induced murine acute myocarditis and chronic fibrosis

Carolina Jaquenod De Giusti [a], Agustín E. Ure [a], Leonardo Rivadeneyra [b], Mirta Schattner [b], Ricardo M. Gomez [a,*]

[a] Instituto de Biotecnología y Biología Molecular, CONICET-UNLP, La Plata, Argentina
[b] Instituto de Medicina Experimental, CONICET-ANM, Argentina

ARTICLE INFO

Article history:
Received 9 January 2015
Received in revised form 11 May 2015
Accepted 12 May 2015
Available online 20 May 2015

Keywords:
Coxsackievirus B3
Myocarditis
Fibrosis
Macrophages
Galectin 3

ABSTRACT

Macrophage influx and galectin 3 production have been suggested as major players driving acute inflammation and chronic fibrosis in many diseases. However, their involvement in the pathogenesis of viral myocarditis and subsequent cardiomyopathy are unknown. Our aim was to characterise the role of macrophages and galectin 3 on survival, clinical course, viral burden, acute pathology, and chronic fibrosis in coxsackievirus B3 (CVB3)-induced myocarditis. Our results showed that C3H/HeJ mice infected with CVB3 and depleted of macrophages by liposome-encapsulated clodronate treatment compared with infected untreated mice presented higher viral titres but reduced acute myocarditis and chronic fibrosis, compared with untreated infected mice. Increased galectin 3 transcriptional and translational expression levels correlated with CVB3 infection in macrophages and in non-depleted mice. Disruption of the galectin 3 gene did not affect viral titres but reduced acute myocarditis and chronic fibrosis compared with C57BL/6J wild-type mice. Similar results were observed after pharmacological inhibition of galectin 3 with *N*-acetyl-D-lactosamine in C3H/HeJ mice. Our results showed a critical role of macrophages and their galectin 3 in controlling acute viral-induced cardiac injury and the subsequent fibrosis. Moreover, the fact that pharmacological inhibition of galectin 3 induced similar results to macrophage depletion regarding the degree of acute cardiac inflammation and chronic fibrosis opens up the possibility of new pharmacological strategies for viral myocarditis.

1. Introduction

Coxsackievirus B3 (CVB3) is a globally prevalent enterovirus of the Picornaviridae family [1] frequently associated with viral myocarditis (VM) [2,3]. While acute VM is typically self-limiting in most individuals, the development of severe heart muscle injury and/or its persistence sustained by post-viral immune-mediated responses, may lead to dilated cardiomyopathy (DCM), and heart failure (HF) in others [3]. DCM is characterised by left ventricular dilatation, decreased ejection fraction, and a depressed wall motion. DCM is attributed, among other factors, to pathological collagen deposition leading to interstitial fibrosis and finally to cardiac dysfunction in a process that may take years or even decades [4]. The mechanisms underlying the pathogenesis of VM, and the cellular and molecular events that link VM to DCM are not well established. Furthermore, therapies for VM are not specific and are directed to supportive care of HF [5]. The last stage of inflammatory heart disease resulting in HF with transplantation as a frequent therapeutic option, is a major healthcare burden worldwide [3].

The CVB3-murine model has provided significant insights into the pathogenesis of VM because it shares many biological parameters of acute and chronic CVB3-induced heart diseases in humans [2,6]. Significant morbidity, mortality and acute myocarditis may be observed during the first days post-infection (dpi) [3] followed by a remarkable extracellular matrix remodelling with fibrosis at 30 dpi [7]. A direct role for virus replication as well as several immune-mediated mechanisms [2,3] have been involved in myocardial disease induced by CVB3.

Although in the steady state most macrophages derive from local progenitors, tissue inflammation changes the source of macrophages. During inflammation, most macrophages derive from inflammatory monocytes that are recruited to the site of inflammation from the blood pool [8] where, following conditioning by local factors, they differentiate into macrophage or dendritic cell populations [9]. In tissues, macrophages further respond to environmental cues with the acquisition of distinct functional phenotypes associated either with a Th1

Abbreviations: VM, viral myocarditis; CVB3, coxsackievirus B3; DCM, dilated cardiomyopathy; HF, heart failure; MOI, multiplicity of infection; LipClod, liposome encapsulated clodronate; Gal-3, galectin 3; dpi, days post-infection; *Lgals3*$^{-/-}$, Gal-3-deficient mice; WT, wild type; ip, intraperitoneally; PFU, plaque forming units; PBS, phosphate buffered saline; Gal-3i, Gal-3 inhibitor, *N*-acetyl-D-lactosamine; IHC, immunohistochemistry; PVDF, polyvinylidene fluoride; RT-PCR, reverse transcription PCR; qRT-PCR, quantitative RT-PCR; CCL-2, chemokine (C–C motif) ligand 2; cTnI, cardiac troponin I; αSMA, α-smooth muscle actin; proCol I, proCollagen type I; ANP, atrial natriuretic peptide/natriuretic peptide type A; BNP, brain natriuretic peptide/natriuretic peptide type B; SCID, severe combined immunodeficiency.

* Corresponding author at: IBBM, CONICET-UNLP, Calle 49 y 115, 1900 La Plata, Argentina. Tel.: +54 221 422 6977; fax: +54 221 422 4967.
E-mail address: rmg1426@gmail.com (R.M. Gomez).

http://dx.doi.org/10.1016/j.yjmcc.2015.05.010
0022-2828/

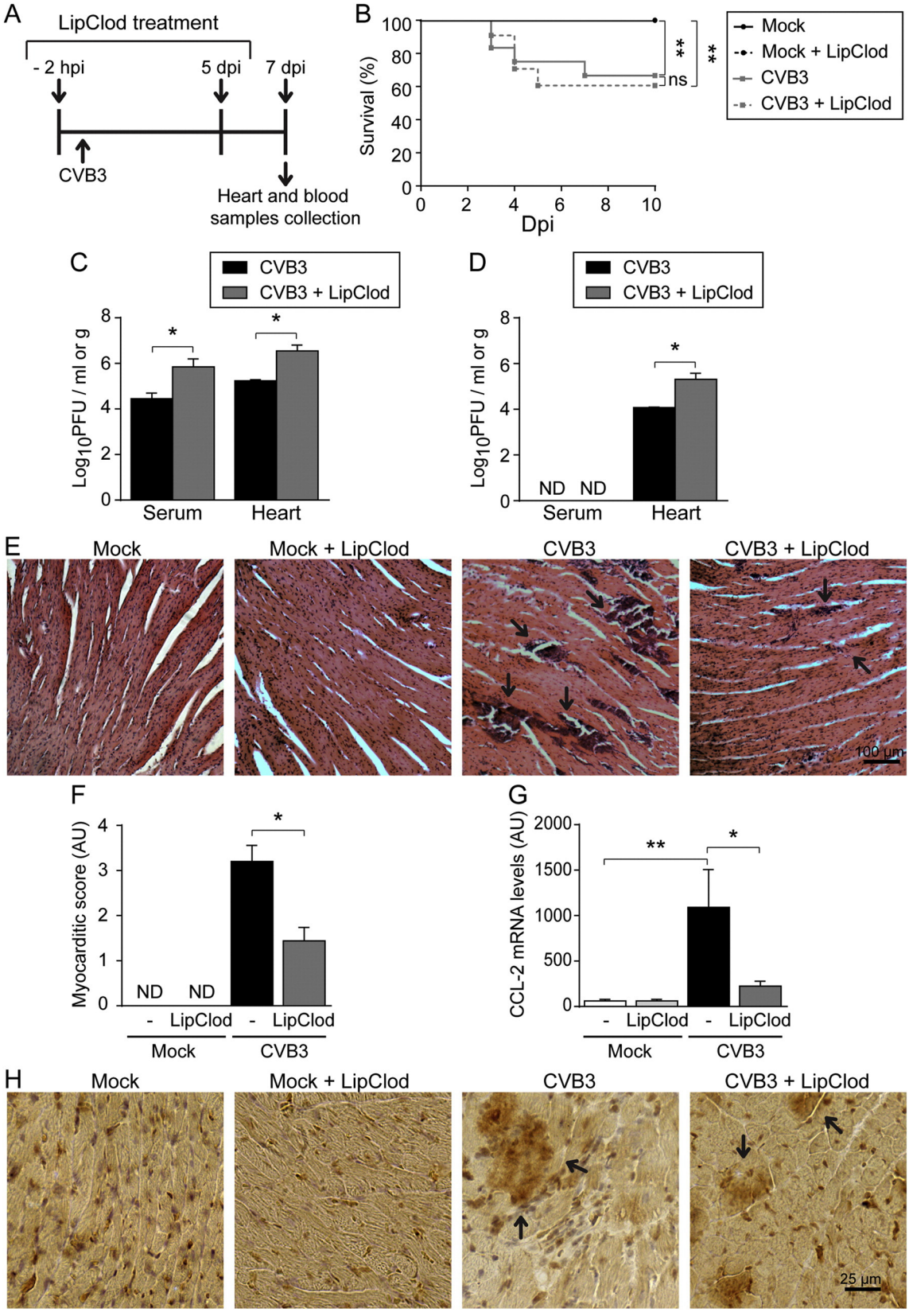

Fig. 1. Depletion of macrophages results in higher viral titres and reduced acute myocarditis. A) Treatment scheme for intraperitoneal (ip) depletion and infection in all groups (Mock, Mock + LipClod, CVB3 and CVB3 + LipClod) of C3H/HeJ mice. B) Percentage of survival in all groups of mice (n = 11–12). C) Viral titres in the serum and heart from all groups of mice at 3 days post-infection (dpi) (n = 6). D) Viral titres in the serum and heart from all groups of mice at 7 dpi (n = 6). E) Representative haematoxylin–eosin staining of the hearts from all groups of mice at 7 dpi. Arrows indicate myocarditic foci. F) Myocarditic score of all groups of mice at 7 dpi (n = 6). G) qRT-PCR analysis of CCL-2 mRNA in heart samples at 7 dpi (n = 6). H) Immunostaining with an antibody against F4/80^{+} cells (macrophages) in heart sections of all groups of mice at 7 dpi. Arrows indicate positive staining. AU: arbitrary units; ND: non-detectable; ns: not significant; $^{*}P < 0.05$; $^{**}P < 0.01$.

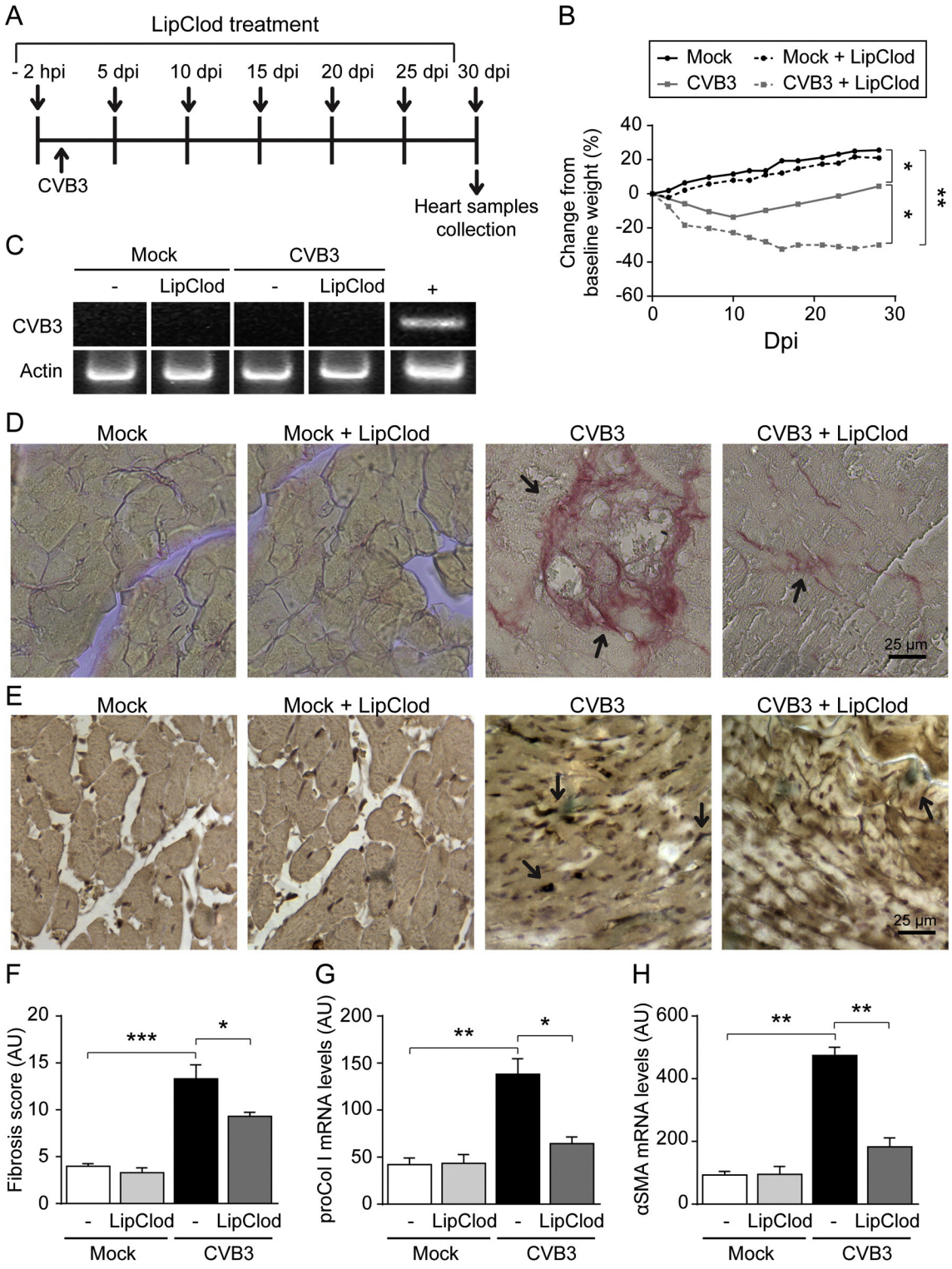

Fig. 2. Depletion of macrophages results in reduced chronic fibrosis. A) Treatment scheme for intraperitoneal (ip) depletion and infection in (Mock, Mock + LipClod, CVB3 and CVB3 + LipClod) groups of C3H/HeJ mice. B) Percentage of body weight change in all groups of mice (n = 6). C) Representative RT-PCR analysis of CVB3 persistence in the hearts of all groups of mice. Actin was used as housekeeping control (n = 6). D) Picrosirius red for collagen staining of heart sections of all groups of mice at 30 dpi. Arrows indicate collagen staining. E) Immunostaining with an antibody against αSMA (myofibroblasts) in heart sections of all groups of mice at 30 dpi. Arrows indicate positive staining. F) Fibrosis score of all 4 groups of mice at 30 dpi (n = 6). G) qRT-PCR analysis of proCol I mRNA in heart samples from all groups of mice at 30 dpi (n = 6). H) qRT-PCR analysis of αSMA mRNA in heart samples from all groups at 30 dpi (n = 6). AU: arbitrary units; ns: not significant; $^{*}P < 0.05$; $^{**}P < 0.01$; $^{***}P < 0.001$.

response, and strong microbicidal activity in acute infections [10]; or with the expression of scavenging and other molecules related to a Th2 response, promotion of tissue remodelling and parasite containment in the chronic stages [11]. The role of monocytes and derived macrophages in many diseases has been clarified by their specific depletion using liposome encapsulated clodronate (LipClod) [12], but their role remains unknown in CVB-induced myocarditis.

Macrophages, cardiac myocytes and fibroblasts can be infected by CVB3 *in vitro*. Fibroblasts are more susceptible to infection compared with myocytes and macrophages, but while myocytes express almost

no cytokines in response to infection, fibroblasts and macrophages express many molecules that may modulate the inflammatory process [13,14]. Interestingly, it has been shown *in vitro* that macrophages are capable of promoting cardiac fibroblast differentiation into myofibroblasts associated with collagen synthesis [15].

Galectin 3 (Gal-3), the only galectin of the chimera-type in the family of β galactoside binding animal lectins, is highly expressed and secreted by macrophages. It has several associated intracellular and extracellular pathological roles as a regulator of acute and chronic inflammations [16]. It is now known that 30–50% of HF patients have an inherently progressive form of the disease mediated by high levels of Gal-3 [17]. Gal-3 expression and secretion by macrophages are major mechanisms linking macrophage migration to fibroblast activation and myofibroblast accumulation, as demonstrated by the synthesis of α-smooth muscle actin (αSMA), and the induction of significant extracellular matrix remodelling during the progression to cardiac fibrosis associated with HF, a process that could be pharmacologically modulated [18,19]. Although Gal-3 has an assigned role in fibrotic diseases [20], its role in VM has not been investigated.

The aim of the present study was to investigate the role of macrophages and Gal-3 in CVB3-induced acute myocarditis and subsequent chronic cardiac fibrosis.

2. Methods

2.1. Cells and virus

HeLa and J774A.1 cells (ATCC, USA) were maintained as monolayers as previously described [21]. A recombinant CVB3 strain with myocarditic properties was used [22]. Viral stocks, propagation and infectivity titration have been previously described [21]. For viral infection, cells were washed with PBS twice before incubating with the virus at a multiplicity of infection (MOI) of 1 in serum free medium. After 1 h of incubation with virus, cells were washed with PBS twice again and supplemented with a complete culture medium. Mock infection was performed by adding the same volume of non-infected HeLa cell culture supernatant.

2.2. ELISA of Gal-3

Cell supernatant levels of Gal-3 were determined using Mouse GAL-3 DuoSet enzyme-linked immunosorbent assay (ELISA) kit (R&D Systems, USA) for sandwich ELISA, using the standard procedure according to the manufacturer's instructions.

2.3. Animals

Weanling (4–5 weeks old) male C3H/HeJ mice, used for the macrophage depletion and Gal-3 inhibition experiments and originally obtained from Jackson Laboratory (USA), were supplied by the Instituto Biológico Argentino (Buenos Aires). Gal-3-deficient mice (*Lgals3*$^{-/-}$)(B6.Cg-*Lgals3*^{tm1Poi}/J) and their control littermates from the C57BL/6J genetic background, originally obtained from Jackson Laboratory (stock 6338), were supplied by the Instituto de Investigaciones Biotecnológicas (IIB), Universidad Nacional de San Martín (Buenos Aires).

2.4. Experimental design

Mice were injected intraperitoneally (ip) with 0.2 ml of phosphate buffered saline (PBS, Mock) or 0.2 ml of PBS containing 10^4 plaque-forming units (PFU) of CVB3. For macrophage depletion, mice were injected ip with 10 μl/g of animal weight of LipClod (clodronateliposomes.org) 2 h before infection and every 5 days (Mock + LipClod and CVB3 + LipClod groups) [12]. For Gal-3 inhibition, mice were injected ip with 5 μg/g of animal weight of *N*-acetyl-D-lactosamine (Gal-3i, Carbosynth, UK) 2 h before infection and every 2 days (Mock + Gal-3i and CVB3 + Gal-3i groups) [23]. Mice were monitored and weighed daily and euthanized by CO_2 overdose at 3, 7 and 30 dpi (6 mice were used for each time point; Supplementary Fig. 1) and their blood and hearts were collected. Routinely, the hearts were spliced in half along the long axis, and one part was frozen at −80 °C for further studies and the other was fixed in 4% paraformaldehyde. The animal experiments were conducted under the approval of the Ethical Research Committee, Facultad de Ciencias Exactas, Universidad Nacional de La Plata. Very sick animals were euthanized by CO_2 overdose. All animals received water and food *ad libitum*.

2.5. Histopathology and immunohistochemistry

Heart samples were processed for routine histology and used to create a myocarditis score as previously described [21]. The picrosirius red technique for collagen staining was carried out as previously described [7]. Digital image analysis was used to quantify the amount of red-stained collagen using a Nikon E200 microscope with a Tucsen TCC 5.0 digital camera and the software provided by the manufacturer. The immunostaining procedure has been previously described [24] using a mouse monoclonal anti αSMA (Dako, USA), a rat monoclonal anti Gal-3 (Clone M3/38, ATCC) and a mouse monoclonal anti-macrophage F4/80 [25] (Novus Biologicals, USA) antibodies.

2.6. Immunoblotting

Immunoblotting was performed as previously described [26]. Tissue or cell samples were processed, separated by SDS-PAGE and electrotransferred to polyvinylidene fluoride (PVDF) membranes. Membranes were incubated with mouse monoclonal anti-actin (GenScript, USA), or the already described anti-Gal-3 and, after washing, with anti-mouse-HRP (Santa Cruz Biotechnology, USA) or anti-rat biotinylated (Dako) followed by streptavidin HRP (Dako). Bands were detected by enhanced chemiluminescence (Amersham, USA) and quantified using LabWorks™ 4.6 (Image Acquisition and Analysis Software).

2.7. RNA isolation, RT-PCR and real-time PCR

Total RNA was isolated from heart samples or cells collected in Tri Reagent (GenBiotech, Argentina) using a Bio-Gen PRO200 homogeniser, as recommended by the manufacturer. The procedure for cDNA synthesis was performed as previously described [26]. The real time PCR (qPCR) studies were performed with a Line-Gene K instrument and software (Bioer) as previously described [26]. Each sample was analysed in triplicate. Normalised expression values were calculated from absolute quantities of the gene of interest and a housekeeping gene.

Fig. 3. Enhanced cardiac Gal-3 expression in CVB3 infection of macrophages and in acute and chronic myocarditis. A) qRT-PCR analysis of Gal-3 mRNA in J774A.1 cells at 1 dpi (n = 6). B) Representative immunoblot of Gal-3 from J774A.1 cells at 1 dpi. Actin was used as loading control. C) Quantitative measurement of Gal-3 density band from J774A.1 cells at 1 dpi (n = 6). D) ELISA measurement of Gal-3 protein levels in the supernatants of J774A.1 cells at 1 dpi (n = 6). E) Immunostaining of heart sections with an antiserum against Gal-3 of all groups (Mock, Mock + LipClod, CVB3 and CVB3 + LipClod) of mice at 7 dpi. Arrows indicate positive staining. F) qRT-PCR analysis of Gal-3 mRNA in heart samples of all groups of mice at 7 dpi (n = 6). G) Representative immunoblot of Gal-3 from cardiac samples of all groups of mice at 7 dpi. Actin was used as loading control. H) Quantitative measurement of Gal-3 density band from all groups of mice at 7 dpi (n = 6). I) Immunostaining of heart sections with an antiserum specific to Gal-3 from all groups of mice at 30 dpi. Arrows indicate positive staining. J) qRT-PCR analysis of Gal-3 mRNA in heart samples of all 4 groups of mice at 30 dpi (n = 6). K) Representative immunoblot of Gal-3 from cardiac samples of all groups of mice at 30 dpi. Actin was used as loading control. L) Quantitative measurement of Gal-3 density band from all groups of mice at 30 dpi (n = 6). AU: arbitrary units; $^{*}P < 0.05$; $^{**}P < 0.01$.

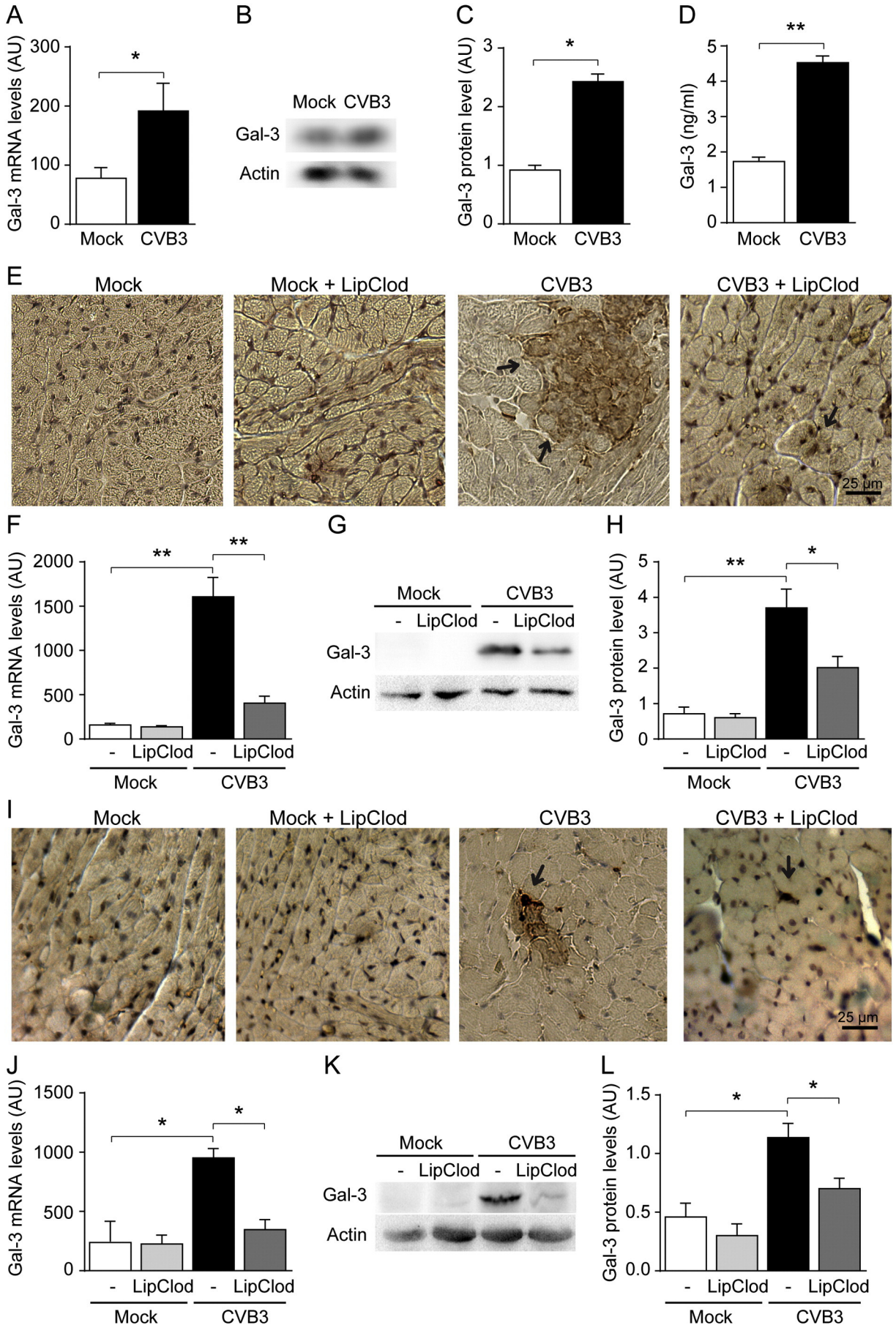
A
Gal-3 mRNA levels (AU)
300
200
100
0
*
Mock
CVB3
B
Mock CVB3
Gal-3
Actin
C
Gal-3 protein level (AU)
3
2
1
0
*
Mock
CVB3
D
Gal-3 (ng/ml)
5
4
3
2
1
0
**
Mock
CVB3
E
Mock
Mock + LipClod
CVB3
CVB3 + LipClod
25 µm
F
Gal-3 mRNA levels (AU)
2000
1500
1000
500
0
**
**
- LipClod - LipClod
Mock
CVB3
G
Mock
CVB3
- LipClod - LipClod
Gal-3
Actin
H
Gal-3 protein level (AU)
5
4
3
2
1
0
**
*
- LipClod - LipClod
Mock
CVB3
I
Mock
Mock + LipClod
CVB3
CVB3 + LipClod
25 µm
J
Gal-3 mRNA levels (AU)
1500
1000
500
0
*
*
- LipClod - LipClod
Mock
CVB3
K
Mock
CVB3
- LipClod - LipClod
Gal-3
Actin
L
Gal-3 protein levels (AU)
1.5
1.0
0.5
0.0
*
*
- LipClod - LipClod
Mock
CVB3

2.8. Statistical analysis

Data were expressed as the mean + S.E.M. and were analysed by one-way analysis of variance (ANOVA) followed by Bonferroni multiple comparison test to determine significant differences between groups. For survival studies data were analysed by Log-rank (Mantel–Cox) test. $P < 0.05$ were considered statistically significant.

3. Results

3.1. Macrophage depletion increased viral replication but reduced acute myocarditis

In order to clarify the role of macrophages in acute viral myocarditis, survival, viral titres and cardiac pathology were studied in infected C3H/HeJ mice depleted or not of macrophages by LipClod treatment (Fig. 1A). The CVB3 and CVB3 + LipClod mice showed 67% and 61% survival rate, respectively, in contrast with the 100% rate of survival of the uninfected controls (Fig. 1B, $P < 0.01$ *versus* control mice, n = 11–12). No more deaths were observed after 7 dpi. Viral burden at 3 dpi was significantly increased in the serum and hearts of CVB3 + LipClod mice compared to the CVB3 group (Fig. 1C, $P < 0.05$, n = 6).

At 7 dpi, no virus was detected in serum samples, but the difference in the hearts persisted (Fig. 1D, $P < 0.05$, n = 6). The histopathological analysis (Fig. 1E) showed an absence of abnormalities in uninfected mice. In contrast, CVB3-infected mice showed typical multifocal myocarditis that was significantly reduced in CVB3 + LipClod mice, scoring 3.20 ± 0.36 and 1.44 ± 0.30, respectively (Fig. 1F, $P < 0.05$, n = 6), a result sustained by the mRNA levels of CCL-2, used as an inflammatory marker (Fig. 1G, $P < 0.01$ CVB3 *versus* control mice and $P < 0.05$ between CVB3 and CVB3 + LipClod mice, n = 6). The immunostaining of marker F4/80 revealed no macrophage infiltration in the controls but a significant infiltration associated with the myocarditic foci in the CVB3 group that was markedly reduced in CVB3 + LipClod mice (Fig. 1H).

Taken together, our results indicate that macrophage depletion results in an increased viral cardiac burden but reduced macrophage cardiac infiltration and myocarditis.

3.2. Depletion of macrophages resulted in reduced fibrosis

To study how macrophage depletion affects the progression of viral myocarditis, the same experimental design used to study acute myocarditis was used for chronicity (Fig. 2A). Body weight, used as a clinical parameter, showed progressive increase over time in uninfected controls. In contrast, the CVB3-infected animal groups showed a marked decrease in the first 10 dpi. However, the CVB3-infected mice then started to gain weight and ended at a weight close to that of the controls, while no such gain was observed in the CVB3 + LipClod group, whose weight at the end of the experiment was 75% of the original value (Fig. 2B, $P < 0.05$ *versus* CVB3 infected mice, $P < 0.01$ *versus* controls, n = 6). In order to study whether macrophage depletion resulted in viral RNA persistence, CVB3 RNA was analysed in heart tissue samples at 30 dpi. As shown in Fig. 2C, no viral RNA was detected in any samples suggesting that macrophages are not essential for the clearance of infected cardiomyocytes. To analyse whether macrophage depletion modulated the cardiac fibrosis that follows CVB3-induced myocarditis, heart samples collected at 30 dpi were stained for collagen with picrosirius red (Fig. 2D). Neither control groups exhibited collagen deposits. In contrast, CVB3-infected mice had several foci of collagen deposits in the hearts that were lower in number and size in the CVB3 + LipClod group. The digital analysis confirmed these observations scoring 3.90 ± 0.27, 3.30 ± 0.51, 13.31 ± 1.48 and 9.31 ± 0.435 for Mock, Mock + LipClod, CVB3 and CVB3 + LipClod, respectively (Fig. 2F, $P < 0.001$ and $P < 0.05$ compared CVB3 to both controls and to CVB3 + LipClod, respectively, n = 6), assigning a significant role of macrophages in chronic fibrosis. To determine whether macrophage depletion modifies the fibroblast activation process, we next studied the immunostaining of αSMA protein present in activated fibroblasts (myofibroblasts) (Fig. 2E). As expected, CVB3-infected mice showed many positive cells, most related to the fibrotic foci, in accordance with the degree of fibrosis observed. Interestingly, CVB3 + LipClod mice showed reduced myofibroblast activation. These results were sustained by qPCR analysis of mRNA levels of proCollagen type I (proCol I) (Fig. 2G, $P < 0.01$ *versus* control mice and $P < 0.05$ *versus* CVB3 + LipClod mice, n = 6) and αSMA (Fig. 2H, $P < 0.01$ *versus* control mice and CVB3 + LipClod mice groups, n = 6).

These results strongly suggest that macrophages are important for cardiac fibroblast activation in the progression of CVB3-induced myocarditis to chronic fibrosis.

3.3. Gal-3 was highly expressed by macrophages and in acute and chronic CVB3-induced myocarditis

In order to study Gal-3 induction in macrophages infected with CVB3, we studied Gal-3 expression levels in the murine macrophage cell line J774A.1. Results showed increased Gal-3 expression levels at both transcriptional (Fig. 3A, $P < 0.05$ *versus* mock infected cells, n = 6) and translational levels (Figs. 3C–D, $P < 0.05$ *versus* mock infected cells, n = 6). Secretion of Gal-3 measure in the supernatants of mock and CVB3 infected cells by ELISA showed increased Gal-3 secretion in CVB3 infected cells (Fig. 3D, $P < 0.01$ *versus* mock infected cells, n = 6). Next, we studied Gal-3 expression levels in the acute phase of VM. The analysis of Gal-3 immunostaining distribution showed many Gal-3-positive cells in the hearts of the CVB3 group mainly associated to the cell exudate, which were drastically reduced in the CVB3 + LipClod mice (Fig. 3E). This result was confirmed at both transcriptional (Fig. 3F, $P < 0.01$ *versus* all groups, n = 6) and translational levels (Figs. 3G–H, $P < 0.01$ *versus* controls and $P < 0.05$ *versus* CVB3 + LipClod mice, n = 6). Taking into account that Gal-3 has also been associated with tissue repair and remodelling [27], we also studied Gal-3 expression during chronic myocarditis. The immunostaining showed less Gal-3-positive cells than in acute phase, some with less intensity and not always associated to focal fibrosis in the CVB3 infected mice, which became minimal in all other groups (Fig. 3I). Transcript and protein analysis supported these observations (Figs. 3J–L, $P < 0.05$ CVB3 *versus* control and CVB3 + LipClod groups, n = 6). These data point out that CVB3 infection triggers Gal-3 expression in macrophages *in vitro* and cardiac Gal-3 expression, and strongly suggest that macrophages are the main source of Gal-3 in acute and chronic myocarditis, but perhaps other cells also express Gal-3 in the chronic phase of VM.

3.4. Gal-3 disruption reduces acute inflammation

In order to study the role of Gal-3 in CVB3-induced acute myocarditis, C57BL/6J *Lgals3*$^{-/-}$ and their control littermate mice were used for a comparative study. There was a survival rate of 75% and 70% in the wild type (WT)- *versus Lgals3*$^{-/-}$-infected mice, respectively (Fig. 4A, $P < 0.01$ *versus* control mice, n = 10–12). No more deaths were observed after 7 dpi. Gal-3 disruption had no effect on viral burden in the serum or heart at 3 and 7 dpi (Figs. 4B and C, respectively, n = 6). No viral RNA was detected in the hearts of infected mice at 30 dpi, indicating that Gal-3 disruption did not affect viral clearance (data not shown). The histopathological analysis showed a slightly reduced multifocal myocarditis in CVB3-infected mice compared with C3H/HeJ mice (in accordance with a previous published work [28]), which was even more reduced in the CVB3-infected *Lgals3*$^{-/-}$ mice (Fig. 4D), scoring 2.16 ± 0.16 and 1.04 ± 0.16, respectively (Fig. 4E, $P < 0.05$, n = 6). This result was confirmed by the mRNA levels of the inflammatory marker CCL-2 (Fig. 4F, $P < 0.05$ WT- *versus Lgals3*$^{-/-}$-infected mice, n = 6). Similar to the

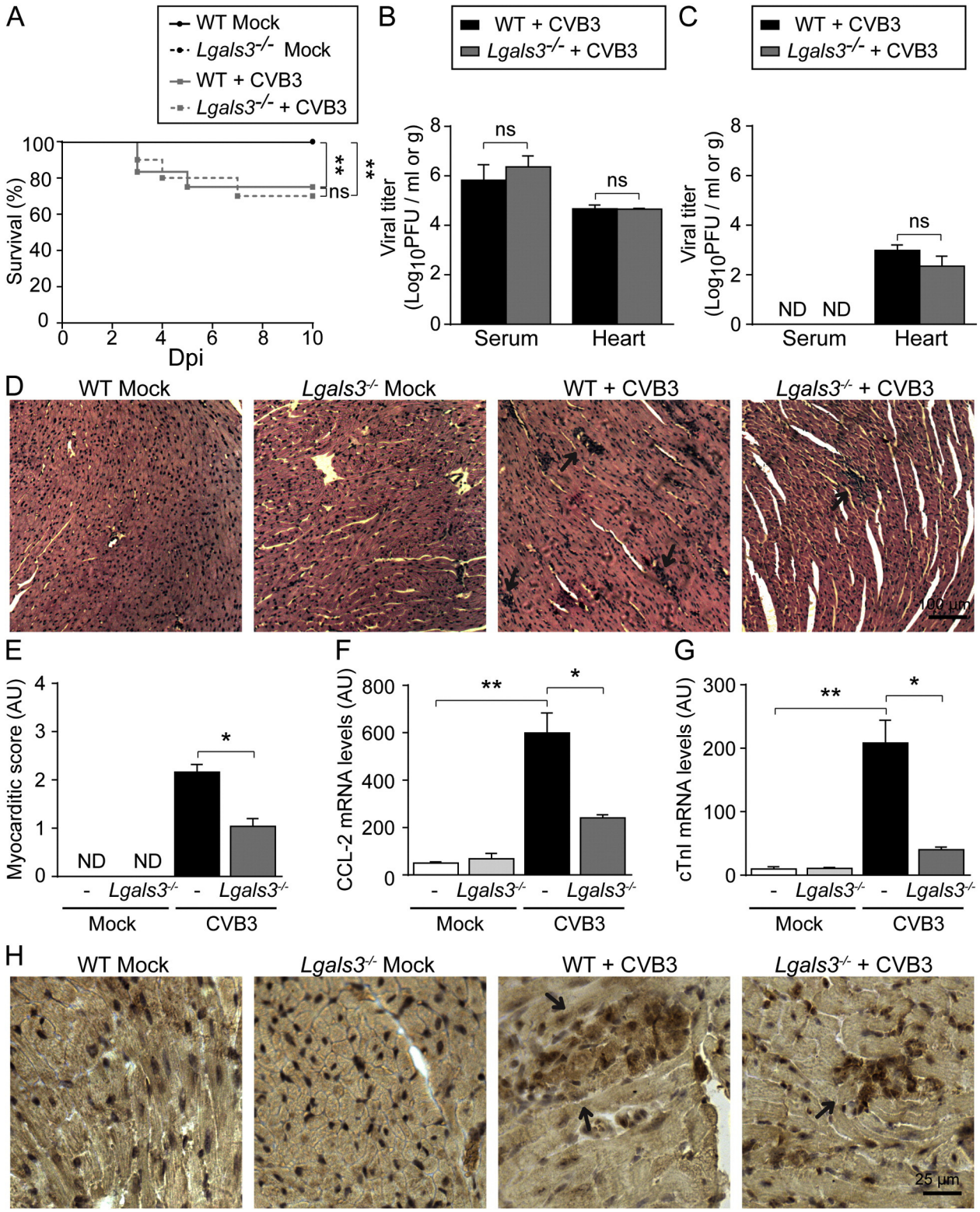

Fig. 4. Genetic disruption of Gal-3 results in similar viral titres but reduced acute myocardial damage. A) Percentage of survival was registered in all groups (Mock, Mock *Lgals3*$^{-/-}$, CVB3 and *Lgals3*$^{-/-}$ + CVB3) of C57BL/6J mice (n = 10–12). B) Viral titres in the serum and heart from all groups of mice at 3 dpi (n = 6). C) Viral titres in the serum and heart from all groups of mice at 7 dpi (n = 6). D) Representative haematoxylin–eosin staining of the hearts from all groups of mice at 7 dpi. Arrows indicate myocarditic foci. E) Myocarditic score of all groups of mice at 7 dpi (n = 6). F) qRT-PCR of CCL-2 mRNA in heart samples from all groups of mice at 7 dpi (n = 6). G) qRT-PCR analysis of cardiac troponin I (cTnI) mRNA in heart samples from all groups of mice at 7 dpi (n = 6). H) Immunostaining for macrophages with an antiserum specific to F4/80^{+} on heart sections of all groups of mice at 7 dpi. Arrows indicate positive staining. AU: arbitrary units; ND: non-detectable; ns: not significant; $^{*}P < 0.05$; $^{**}P < 0.01$.

results obtained in C3H/HeJ mice, immunostaining showed that CVB3 infection induced intensive macrophage infiltration, which was slightly reduced in *Lgals3*$^{-/-}$ mice (Fig. 4H).

Taken together, our results indicate that Gal-3 has no role in CVB3 replication but is involved in the heart tissue inflammation and cardiomyocyte damage present in the acute phase of CVB3-induced myocarditis.

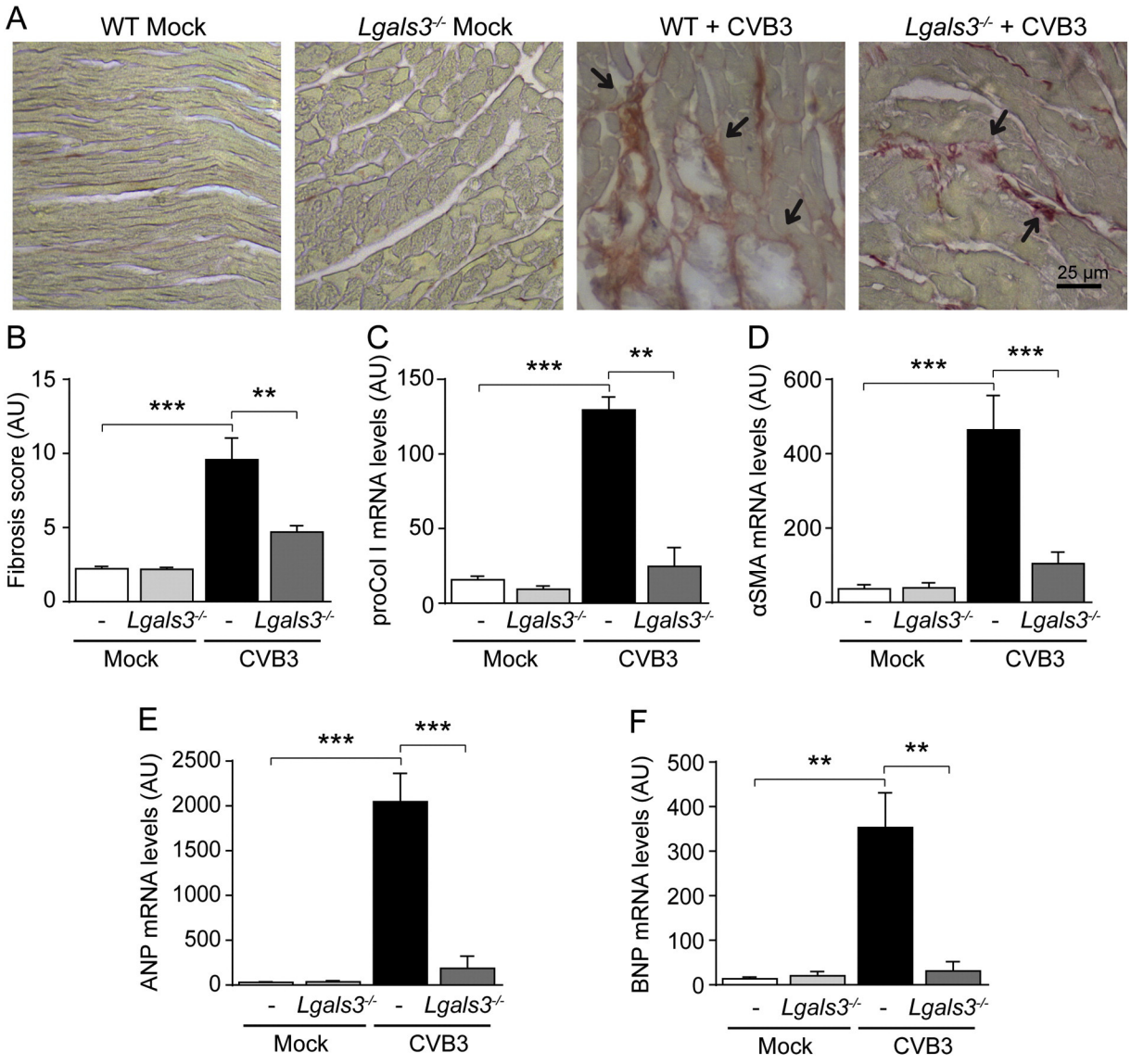

Fig. 5. Genetic disruption of Gal-3 results in reduced fibrosis. A) Collagen staining with picrosirius red in the hearts of all groups (Mock, Mock *Lgals3*$^{-/-}$, CVB3 and *Lgals3*$^{-/-}$ + CVB3) of C57BL/6J mice at 30 dpi. Arrows indicate collagen staining. B) Fibrosis score of all groups of mice at 30 dpi (n = 6). C) qRT-PCR analysis of proCol I mRNA in heart samples from all groups of mice at 30 dpi (n = 6). D) qRT-PCR analysis of αSMA mRNA in heart samples from all groups of mice at 30 dpi (n = 6). E) qRT-PCR analysis of natriuretic peptide type A (ANP) mRNA in heart samples from all groups at 30 dpi (n = 6). F) qRT-PCR analysis of natriuretic peptide type B (BNP) mRNA in heart samples from all groups at 30 dpi (n = 6). AU: arbitrary units; $^{**}P < 0.01$; $^{***}P < 0.001$.

3.5. Gal-3 disruption reduced fibrosis

We also characterised the role of Gal-3 in the chronic phase of CVB3-induced murine myocarditis by analysing fibrosis. WT-infected mice had high collagen staining, which was significantly reduced in infected *Lgals3*$^{-/-}$ mice and minimal in uninfected controls (Fig. 5A), scoring 9.58 ± 1.46, 4.70 ± 0.43, 2.40 ± 0.27, and 2.30 ± 0.51, respectively (Fig. 5B) ($P < 0.001$ *versus* control mice and $P < 0.01$ between infected mice, n = 6). These results were confirmed by mRNA expression levels of proCol I (Fig. 5C) and αSMA (Fig. 5D) ($P < 0.01$ and $P < 0.001$ between WT CVB3 *versus* all other mice, n = 6). Considering that increased collagen content results in reduced cardiac contractility, we next decided to test whether the reduction in fibrosis observed in infected *Lgals3*$^{-/-}$ mice would result on improved cardiac outcome. For this purpose, we measured mRNA levels of A and B-type natriuretic peptide (ANP and BNP, respectively) that are markers of cardiac dysfunction [29,30]. Results showed increased levels of both markers in the WT-infected mice that were significantly reduced in *Lgals3*$^{-/-}$ infected mice (Fig. 5E, $P < 0.001$ between WT-infected mice *versus* all other mice, n = 6 and Fig. 5F, $P < 0.01$ between WT-infected mice *versus* all other mice, n = 6).

In summary, Gal-3 genetic disruption results in decreased fibrosis and improved cardiac function.

3.6. Gal-3 inhibition reduced acute myocarditis

To further clarify the role of extracellular Gal-3 in acute VM, mortality, viral titres and cardiac pathology were examined in CVB3-infected mice treated or not with Gal-3i (Fig. 6A). The CVB3 and CVB3 + Gal-3i mice showed 70 and 75% of survival, respectively (Fig. 6B, n = 10–12). As expected, Gal-3 inhibition did not alter Gal-3 mRNA expression levels (Fig. 6C, n = 6). As shown in Figs. 6D–E, Gal-3 inhibition had no effect on viral burden in the serum or hearts of infected mice at 3 and 7 dpi. No viral RNA was detected in the hearts of infected mice at 30 dpi, indicating that Gal-3 inhibition did not affect viral clearance (data not shown). However, while multifocal myocarditis was observed in CVB3-infected mice, CVB3 + Gal-3i mice showed reduced tissue damage (Fig. 6F), scoring

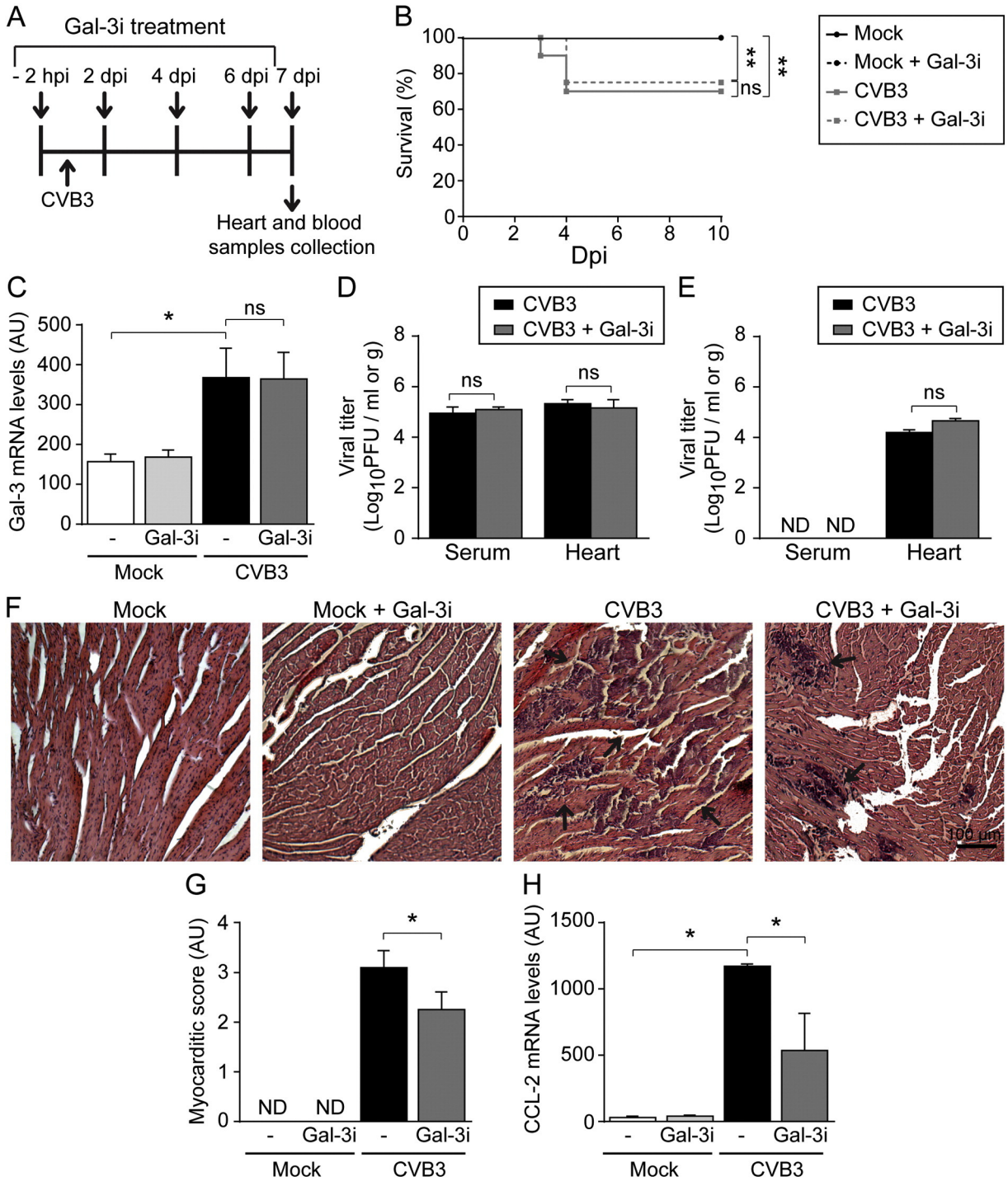

Fig. 6. Pharmacological inhibition of Gal-3 did not modify viral burden but reduced acute myocarditis. A) Gal-3 inhibitor (Gal-3i) injection and infection scheme in C3H/HeJ mice. B) Percentage of survival in all groups (Mock, Mock + Gal-3i, CVB3, and CVB3 + Gal-3i) of mice (n = 10–12). C) qRT-PCR analysis of Gal-3 mRNA in heart samples from all groups of mice at 7 dpi (n = 6). D) Viral titres in the serum and heart from all groups of mice at 3 dpi (n = 6). E) Viral titres in the serum and heart from all groups of mice at 7 dpi (n = 6). F) Representative haematoxylin–eosin staining of the hearts from all groups of mice at 7 dpi. Arrows indicate myocarditic foci. G) Myocardial damage score of all groups of mice at 7 dpi (n = 6). H) qRT-PCR analysis of CCL-2 mRNA in heart samples from all groups of mice at 7 dpi (n = 6). I) qRT-PCR analysis of cardiac troponin I (cTnI) mRNA in heart samples from all groups of mice at 7 dpi (n = 6). AU: arbitrary units; ND: non-detectable; ns: not significant; $^{*}P < 0.05$.

3.10 ± 0.34 and 2.20 ± 0.36, respectively (Fig. 6G, $P < 0.05$, n = 6), and decreased mRNA levels of the inflammatory marker CCL-2 (Fig. 6H, $P < 0.05$, n = 6).

Thus, pharmacological blockade of Gal-3 does not affect viral replication, but reduces the heart tissue inflammation and cardiomyocyte damage present in the acute phase of CVB3-induced acute myocarditis.

3.7. Gal-3 inhibition improved body weight recovery and reduced fibrosis

Finally, we analysed the chronic phase of CVB3 infection in Gal-3i treated mice (Fig. 7A). Treatment resulted in a significant recovery of body weight of infected animals (Fig. 7B, $P < 0.05$, n = 6). In addition, Gal-3 inhibition reduced the cardiac fibrosis that followed CVB3-induced myocarditis (Fig. 7C), scoring 3.98 ± 0.27, 3.75 ± 0.31,

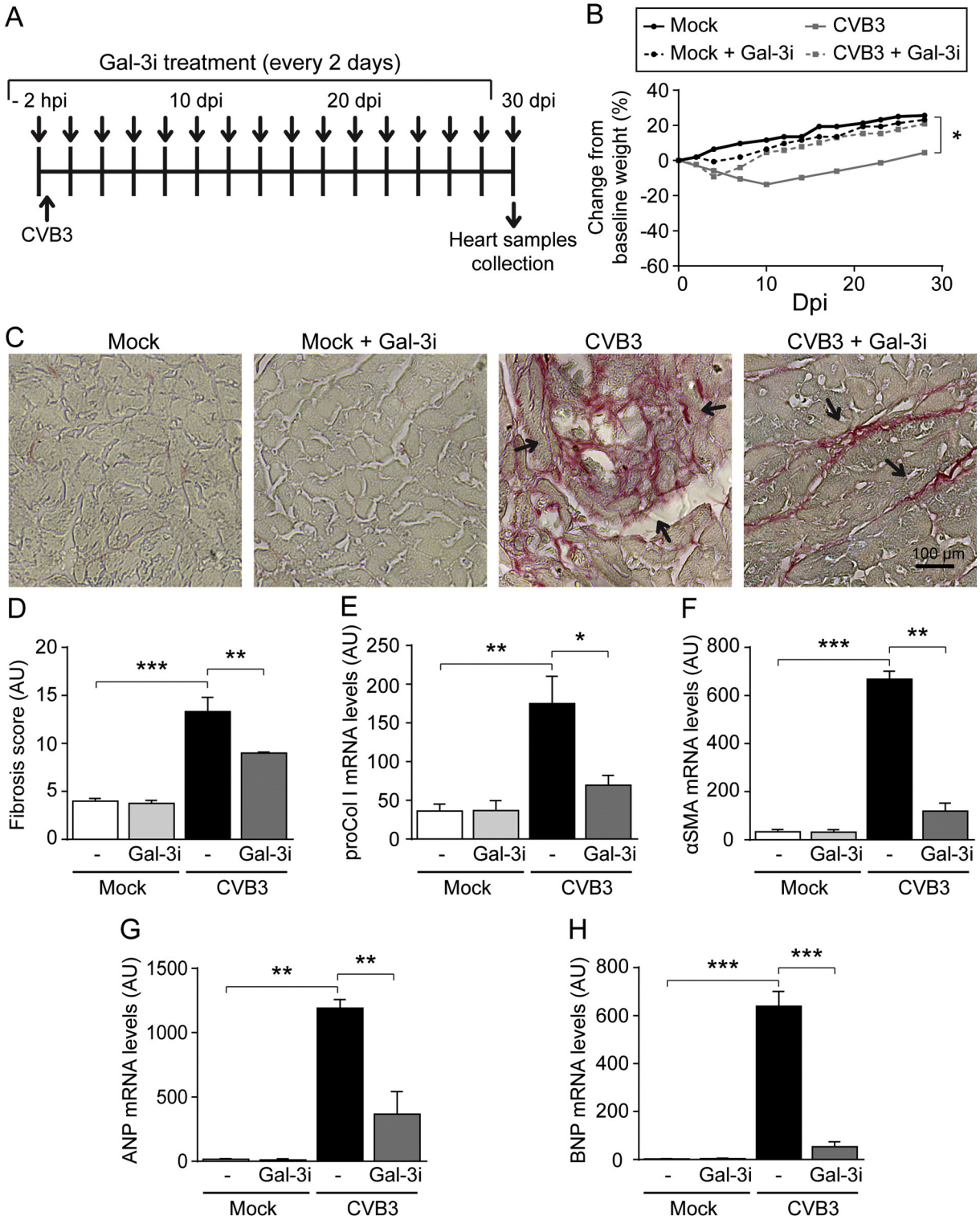

Fig. 7. Pharmacological inhibition of Gal-3 reduces fibrosis. A) Gal-3i injection and infection scheme in C3H/HeJ mice. B) Percentage of body weight change in all groups (Mock, Mock + Gal-3i, CVB3, and CVB3 + Gal-3i) of mice (n = 6). C) Picrosirius red for collagen staining from hearts of all groups of mice at 30 dpi. Arrows indicate collagen staining. D) Fibrosis score of all groups of mice at 30 dpi (n = 6). E) qRT-PCR analysis of proCol I mRNA in heart samples from all groups of mice at 30 dpi (n = 6). F) qRT-PCR analysis of αSMA mRNA in heart samples from all groups of mice at 30 dpi (n = 6). G) qRT-PCR analysis of natriuretic peptide type A (ANP) mRNA in heart samples from all groups at 30 dpi (n = 6). H) qRT-PCR analysis of natriuretic peptide type B (BNP) mRNA in heart samples from all groups at 30 dpi (n = 6). AU: arbitrary units; $^{*}P < 0.05$; $^{**}P < 0.01$; $^{***}P < 0.001$.

13.31 ± 1.48 and 8.99 ± 0.10 for Mock, Mock + Gal-3i, CVB3 and CVB3 + Gal-3i, respectively (Fig. 7D, $P < 0.001$ and <0.01 CVB3 compared to control and to CVB3 + Gal-3i mice, respectively, n = 6). These results were confirmed by mRNA levels of proCol I (Fig. 7E, $P < 0.01$ and $P < 0.05$ compared to control or CVB3 + Gal-3i mice, respectively, n = 6) and αSMA (Fig. 7F $P < 0.001$ and $P < 0.01$ compared to control or CVB3 + Gal-3i mice, respectively, n = 6). To analyse cardiac outcome we measured ANP and BNP mRNA levels. Results showed increased levels of both markers in the CVB3 infected mice and a significant reduction on Gal-3i treated infected mice (Fig. 7G, $P < 0.01$

compared to all groups of mice, and H, $P < 0.01$ compared to all groups of mice, n = 6, respectively).

The results demonstrate that Gal-3 inhibition significantly reduces chronic fibrosis and improves cardiac function in CVB3-induced chronic myocarditis.

4. Discussion

In this study, we investigated the role of macrophages and Gal-3 in the CVB3-induced murine myocarditis model. We demonstrated that macrophages play a critical role in controlling viral replication, acute cardiac inflammation and chronic fibrosis. In addition we showed that CVB3 infection triggers acute and chronic enhanced expressions of Gal-3 in the heart and that genetic disruption or pharmacological inhibition of Gal-3 results in a moderate reduction of acute myocarditis but in a marked decrease of chronic fibrosis without affecting viral replication.

Although we did not find differences in the survival rate between infected untreated animals and those depleted of macrophages, previous work using the CVB3 murine model showed that macrophage depletion increased mice mortality [31]. However, the fact that macrophage depletion was achieved using silica particles, a procedure associated with increased macrophage activation [32], leads to uncertainty regarding the role of macrophages in that study [33].

Our results showed that macrophage depletion results in increased viral titres concomitant with reduced cardiomyocyte necrosis and tissue inflammation. Macrophages are major components of host defence and have been associated with viral clearance from infected tissues in several murine models of acute viral infection, including murine cytomegalovirus [34], West Nile virus [35] and influenza virus [36]. Moreover, macrophage depletion resulted in enhanced influenza virus replication and lung inflammation, indicating that macrophages control influenza virus lung infection and limit the development of tissue injury [37]. In contrast, in myocarditis induced by the picornavirus encephalomyocarditis virus, depletion of macrophages reduced viral burden and pathology suggesting that in this case, macrophages are involved in viral replication and dissemination [38]. In agreement with previous studies where acute necrotic cardiomyocytes were surrounded predominantly by natural killer cells (NK cells), macrophages and T lymphocytes [39,40], our results showed that infiltrating macrophages are mostly related to myocarditic foci. In addition, severe combined immunodeficiency (SCID) mice, which lack functional T and B cells but have functional NK cells and macrophages, showed overwhelming necrotizing myocarditis caused not only by CVB3 [41], but also by the picornavirus Theiler's murine encephalomyelitis virus [42]. However, NK cells seem to play a role in pancreas resistance to CVB infection [43] but do not alter the cardiac viral clearance after its depletion [44], or inhibition [45]. Taken together, it seems that in CVB3-induced myocarditis, cardiac infiltrating macrophages have a major role in the early clearance of infected cardiomyocytes in accordance with the assigned dual role of macrophages not only limiting tissue injury but also increasing tissue damage [46]. The fact that macrophage-depleted mice also presented lower body weight suggests that besides their role in chronic myocarditis, macrophages might have additional roles, controlling viral replication and/or tissue damage in other organs.

Persistence of viral RNA has been involved as a pathogenic mechanism linking acute VM to CMD [5,47]. This persistence was observed only in some strains of mice and was related to the degree of viral burden and the extent of acute necrosis [48]. It involved cardiomyocytes, B cells and macrophages [49]. Although we observed higher viral titres (but less pathology) in macrophage depleted mice, there was an absence of RNA persistence, suggesting that macrophages do not play a role in this pathogenic mechanism.

Several studies have shown macrophages to have an important role in promoting fibrosis [50–52]. Nevertheless, in most of these studies, tissue damage was achieved by drug treatment or mechanical obstruction, not after viral infection, where macrophages are first involved in controlling viral replication and dissemination, a fact that may affect their later roles. In our model, fibrosis was reduced in macrophage-depleted mice, suggesting that macrophages play an important role in promoting heart fibrosis. According to our data, the reduced fibrosis may also be due to the reduced acute tissue damage and inflammation in macrophage-depleted mice.

We also demonstrated that CVB3 murine infection resulted in increased Gal-3 expression at both transcript and translational levels in macrophages and also in the acute and chronic phases of viral myocarditis. We also observed increased Gal-3 secretion by macrophages. The fact that Gal-3 staining was mainly associated with the cell exudate, and that macrophage depletion resulted in a significant reduction of Gal-3 expression strongly suggests that macrophages are the main source of cardiac Gal-3. These observations are in agreement with findings made in hypertrophied hearts where Gal-3 was not detected in cardiomyocytes but it was found in infiltrating cells, mostly macrophages [53].

Several studies showed that Gal-3 has a major role as an acute and chronic inflammatory mediator [16] during parasitic [54], viral [55], or bacterial [56] infections and in chronic fibrosis of the liver [57], kidney [52] and heart [18]. Our data showing that viral burden was similar in the acute phase in *Lgals3*$^{-/-}$ mice compared to WT littermates or mice treated with the Gal-3 inhibitor *N*-acetyl-D-lactosamine, suggesting that Gal-3 has no effect on CVB3 dissemination or replication. These results are in contrast with the reported enhanced infection by herpes simplex virus [58] and human T-cell leukaemia virus [59]. These differences could be associated with the different nature and replicative cycles of these viruses. Interestingly, *Lgals3*$^{-/-}$ mice or Gal-3i-treated mice showed reduced acute inflammation and necrosis, a fact that may be explained by its active role in recruiting inflammatory cells [60,61], including macrophages [20]. In addition, because of the reduced acute inflammation and/or by a more direct role, genetic disruption of Gal-3 or its pharmacological inhibition resulted in reduced fibrosis in the chronic phase of CVB3-induced murine myocarditis. Furthermore, Gal-3 inhibition also resulted in an improved clinical outcome interpreted as an increase in body weight and reduced HF markers. This is in line with the observed reversion of cardiac remodelling after transverse aortic constriction-induced hypertrophy and improvement of left-ventricular function with Gal-3 inhibition [23]. As a limitation of this study, it lacks heart functional data such as haemodynamics and echocardiography. Further studies regarding heart function will be needed in order to confirm our results. Nevertheless, Gal-3 inhibition has been used for fibrosis treatment in several animal models (reviewed in Refs. [62,63]) and it is under clinical trial for the treatment of human idiopathic pulmonary fibrosis (US National Institutes of Health, ClinicalTrials.gov identifier: NCT02257177).

5. Conclusion

Our results show that reduction of CVB3-induced cardiac damage and inflammatory responses, through inhibition of Gal-3, may be achieved with the subsequent reduction of chronic fibrosis, opening the possibility of new therapeutic strategies for human diseases.

Sources of funding

This work was supported by grants from Universidad Nacional de La Plata (X592) and Agencia Nacional de Promoción Científica y Tecnológica (ANPCyT) PICT 2012-0434 (RMG).

Disclosures

All the authors declared no competing interests.

Acknowledgments

We thank Dr. O. Campetella from the Instituto de Investigaciones Biotecnológicas (IIB), UNSAM-CONICET for the generous provision of the *Lgals3*$^{-/-}$ mice.

Appendix A. Supplementary data

Supplementary data to this article can be found online at http://dx.doi.org/10.1016/j.yjmcc.2015.05.010.

References

[1] Stanway G, Brown F, Christian P, Hovi T, Hyypiä T, King AMQ, et al. Picornaviridae. In: Fauquet CM, Mayo MA, Maniloff J, Desselberger U, Ball LA, editors. Virus taxonomy, VIIIth report of the ICTV. London, United Kingdom: Elsevier; 2004. p. 757–78.
[2] Fairweather D, Stafford KA, Sung YK. Update on coxsackievirus B3 myocarditis. Curr Opin Rheumatol 2012;24:401–7.
[3] Andreoletti L. Viral myocarditis: physiopathology and diagnosis. In: Cihakova D, editor. Myocarditis: InTech; 2011.
[4] Szalay G, Sauter M, Haberland M, Zuegel U, Steinmeyer A, Kandolf R, et al. Osteopontin: a fibrosis-related marker molecule in cardiac remodeling of enterovirus myocarditis in the susceptible host. Circ Res 2009;104:851–9.
[5] Kindermann I, Barth C, Mahfoud F, Ukena C, Lenski M, Yilmaz A, et al. Update on myocarditis. J Am Coll Cardiol 2012;59:779–92.
[6] Gauntt C, Huber S. Coxsackievirus experimental heart diseases. Front Biosci 2003;8:e23–35.
[7] Gomez RM, Castagnino CG, Berria MI. Extracellular matrix remodelling after coxsackievirus B3-induced murine myocarditis. Int J Exp Pathol 1992;73:643–53.
[8] Shinagawa H, Frantz S. Cellular immunity and cardiac remodeling after myocardial infarction: role of neutrophils, monocytes, and macrophages. Curr Heart Fail Rep 2015;12:247–54.
[9] Auffray C, Sieweke MH, Geissmann F. Blood monocytes: development, heterogeneity, and relationship with dendritic cells. Annu Rev Immunol 2009;27:669–92.
[10] Mosser DM, Edwards JP. Exploring the full spectrum of macrophage activation. Nat Rev Immunol 2008;8:958–69.
[11] Sica A, Mantovani A. Macrophage plasticity and polarization: in vivo veritas. J Clin Invest 2012;122:787–95.
[12] van Rooijen N, Hendrikx E. Liposomes for specific depletion of macrophages from organs and tissues. Methods Mol Biol 2010;605:189–203.
[13] Heim A, Zeuke S, Weiss S, Ruschewski W, Grumbach IM. Transient induction of cytokine production in human myocardial fibroblasts by coxsackievirus B3. Circ Res 2000;86:753–9.
[14] Lindner D, Li J, Savvatis K, Klingel K, Blankenberg S, Tschope C, et al. Cardiac fibroblasts aggravate viral myocarditis: cell specific coxsackievirus B3 replication. Mediators Inflamm 2014;2014:519528.
[15] Ma F, Li Y, Jia L, Han Y, Cheng J, Li H, et al. Macrophage-stimulated cardiac fibroblast production of IL-6 is essential for TGF beta/Smad activation and cardiac fibrosis induced by angiotensin II. PLoS One 2012;7 e35144.
[16] Liu FT, Rabinovich GA. Galectins: regulators of acute and chronic inflammation. Ann N Y Acad Sci 2010;1183:158–82.
[17] de Boer RA, Lok DJ, Jaarsma T, van der Meer P, Voors AA, Hillege HL, et al. Predictive value of plasma galectin-3 levels in heart failure with reduced and preserved ejection fraction. Ann Med 2011;43:60–8.
[18] de Boer RA, Yu L, van Veldhuisen DJ. Galectin-3 in cardiac remodeling and heart failure. Curr Heart Fail Rep 2010;7:1–8.
[19] Sharma U, Rhaleb NE, Pokharel S, Harding P, Rasoul S, Peng H, et al. Novel anti-inflammatory mechanisms of N-Acetyl-Ser-Asp-Lys-Pro in hypertension-induced target organ damage. Am J Physiol Heart Circ Physiol 2008;294:H1226–32.
[20] Li LC, Li J, Gao J. Functions of galectin-3 and its role in fibrotic diseases. J Pharmacol Exp Ther 2014;351:336–43.
[21] Cifuente JO, Ferrer MF, Jaquenod De Giusti C, Song WC, Romanowski V, Hafenstein SL, et al. Molecular determinants of disease in coxsackievirus B1 murine infection. J Med Virol 2011;83:1571–81.
[22] Knowlton KU, Jeon ES, Berkley N, Wessely R, Huber S. A mutation in the puff region of VP2 attenuates the myocarditic phenotype of an infectious cDNA of the Woodruff variant of coxsackievirus B3. J Virol 1996;70:7811–8.
[23] Yu L, Ruifrok WP, Meissner M, Bos EM, van Goor H, Sanjabi B, et al. Genetic and pharmacological inhibition of galectin-3 prevents cardiac remodeling by interfering with myocardial fibrogenesis. Circ Heart Fail 2013;6:107–17.
[24] Ferrer MF, Pascuale CA, Gomez RM, Leguizamon MS. DTU I isolates of *Trypanosoma cruzi* induce upregulation of galectin-3 in murine myocarditis and fibrosis. Parasitology 2014;141:849–58.
[25] Austyn JM, Gordon S. F4/80, a monoclonal antibody directed specifically against the mouse macrophage. Eur J Immunol 1981;11:805–15.
[26] Negrotto S, Jaquenod De Giusti C, Rivadeneyra L, Ure AE, Mena HA, Schattner M, et al. Platelets interact with coxsackieviruses B and have a critical role in the pathogenesis of virus-induced myocarditis. J Thromb Haemost 2015;13:271–82.
[27] Henderson NC, Sethi T. The regulation of inflammation by galectin-3. Immunol Rev 2009;230:160–71.
[28] Chow LH, Gauntt CJ, McManus BM. Differential effects of myocarditic variants of coxsackievirus B3 in inbred mice. A pathologic characterization of heart tissue damage. Lab Invest 1991;64:55–64.
[29] Takemura G, Fujiwara H, Takatsu Y, Fujiwara T, Nakao K. Ventricular expression of atrial and brain natriuretic peptides in patients with myocarditis. Int J Cardiol 1995;52:213–22.
[30] Fairweather D, Abston ED, Coronado MJ. Biomarkers of heart failure in myocarditis and dilated cardiomyopathy. In: Cihakova D, editor. Myocarditis: InTech; 2011.
[31] Rager-Zisman B, Allison AC. The role of antibody and host cells in the resistance of mice against infection by coxsackie B-3 virus. J Gen Virol 1973;19:329–38.
[32] van Rooijen N, Sanders A. Elimination, blocking, and activation of macrophages: three of a kind? J Leukoc Biol 1997;62:702–9.
[33] Frantz S, Nahrendorf M. Cardiac macrophages and their role in ischaemic heart disease. Cardiovasc Res 2014;102:240–8.
[34] Salazar-Mather TP, Orange JS, Biron CA. Early murine cytomegalovirus (MCMV) infection induces liver natural killer (NK) cell inflammation and protection through macrophage inflammatory protein 1alpha (MIP-1alpha)-dependent pathways. J Exp Med 1998;187:1–14.
[35] Lim JK, Obara CJ, Rivollier A, Pletnev AG, Kelsall BL, Murphy PM. Chemokine receptor Ccr2 is critical for monocyte accumulation and survival in West Nile virus encephalitis. J Immunol 2011;186:471–8.
[36] Aldridge Jr JR, Moseley CE, Boltz DA, Negovetich NJ, Reynolds C, Franks J, et al. TNF/iNOS-producing dendritic cells are the necessary evil of lethal influenza virus infection. Proc Natl Acad Sci U S A 2009;106:5306–11.
[37] Tate MD, Pickett DL, van Rooijen N, Brooks AG, Reading PC. Critical role of airway macrophages in modulating disease severity during influenza virus infection of mice. J Virol 2010;84:7569–80.
[38] Hirasawa K, Tsutsui S, Takeda M, Mizutani M, Itagaki S, Doi K. Depletion of Mac1-positive macrophages protects DBA/2 mice from encephalomyocarditis virus-induced myocarditis and diabetes. J Gen Virol 1996;77(Pt 4):737–41.
[39] Deguchi H, Kitaura Y, Hayashi T, Kotaka M, Kawamura K. Cell-mediated immune cardiocyte injury in viral myocarditis of mice and patients. Jpn Circ J 1989;53:61–77.
[40] Godeny EK, Gauntt CJ. In situ immune autoradiographic identification of cells in heart tissues of mice with coxsackievirus B3-induced myocarditis. Am J Pathol 1987;129:267–76.
[41] Chow LH, Beisel KW, McManus BM. Enteroviral infection of mice with severe combined immunodeficiency. Evidence for direct viral pathogenesis of myocardial injury. Lab Invest 1992;66:24–31.
[42] Gomez RM, Rinehart JE, Wollmann R, Roos RP. Theiler's murine encephalomyelitis virus-induced cardiac and skeletal muscle disease. J Virol 1996;70:8926–33.
[43] Vella C, Festenstein H. Coxsackievirus B4 infection of the mouse pancreas: the role of natural killer cells in the control of virus replication and resistance to infection. J Gen Virol 1992;73:1379–86.
[44] Yuan J, Liu Z, Lim T, Zhang H, He J, Walker E, et al. CXCL10 inhibits viral replication through recruitment of natural killer cells in coxsackievirus B3-induced myocarditis. Circ Res 2009;104:628–38.
[45] Matsui S, Matsumori A, Matoba Y, Uchida A, Sasayama S. Treatment of virus-induced myocardial injury with a novel immunomodulating agent, vesnarinone. Suppression of natural killer cell activity and tumor necrosis factor-alpha production. J Clin Invest 1994;94:1212–7.
[46] Laskin DL, Sunil VR, Gardner CR, Laskin JD. Macrophages and tissue injury: agents of defense or destruction? Annu Rev Pharmacol Toxicol 2011;51:267–88.
[47] Wessely R, Klingel K, Santana LF, Dalton N, Hongo M, Jonathan Lederer W, et al. Transgenic expression of replication-restricted enteroviral genomes in heart muscle induces defective excitation–contraction coupling and dilated cardiomyopathy. J Clin Invest 1998;102:1444–53.
[48] Klingel K, Hohenadl C, Canu A, Albrecht M, Seemann M, Mall G, et al. Ongoing enterovirus-induced myocarditis is associated with persistent heart muscle infection: quantitative analysis of virus replication, tissue damage, and inflammation. Proc Natl Acad Sci U S A 1992;89:314–8.
[49] Klingel K, Stephan S, Sauter M, Zell R, McManus BM, Bultmann B, et al. Pathogenesis of murine enterovirus myocarditis: virus dissemination and immune cell targets. J Virol 1996;70:8888–95.
[50] Duffield JS, Forbes SJ, Constandinou CM, Clay S, Partolina M, Vuthoori S, et al. Selective depletion of macrophages reveals distinct, opposing roles during liver injury and repair. J Clin Invest 2005;115:56–65.
[51] Sung SA, Jo SK, Cho WY, Won NH, Kim HK. Reduction of renal fibrosis as a result of liposome encapsulated clodronate induced macrophage depletion after unilateral ureteral obstruction in rats. Nephron Exp Nephrol 2007;105:e1–9.
[52] Henderson NC, Mackinnon AC, Farnworth SL, Kipari T, Haslett C, Iredale JP, et al. Galectin-3 expression and secretion links macrophages to the promotion of renal fibrosis. Am J Pathol 2008;172:288–98.
[53] Sharma UC, Pokharel S, van Brakel TJ, van Berlo JH, Cleutjens JP, Schroen B, et al. Galectin-3 marks activated macrophages in failure-prone hypertrophied hearts and contributes to cardiac dysfunction. Circulation 2004;110:3121–8.
[54] Breuilh L, Vanhoutte F, Fontaine J, van Stijn CM, Tillie-Leblond I, Capron M, et al. Galectin-3 modulates immune and inflammatory responses during helminthic infection: impact of galectin-3 deficiency on the functions of dendritic cells. Infect Immun 2007;75:5148–57.
[55] Sato S, Ouellet M, St-Pierre C, Tremblay MJ. Glycans, galectins, and HIV-1 infection. Ann N Y Acad Sci 2012;1253:133–48.
[56] Mishra BB, Li Q, Steichen AL, Binstock BJ, Metzger DW, Teale JM, et al. Galectin-3 functions as an alarmin: pathogenic role for sepsis development in murine respiratory tularemia. PLoS One 2013;8 e59616.

[57] Henderson NC, Mackinnon AC, Farnworth SL, Poirier F, Russo FP, Iredale JP, et al. Galectin-3 regulates myofibroblast activation and hepatic fibrosis. Proc Natl Acad Sci U S A 2006;103:5060–5.
[58] Woodward AM, Mauris J, Argueso P. Binding of transmembrane mucins to galectin-3 limits herpesvirus 1 infection of human corneal keratinocytes. J Virol 2013;87:5841–7.
[59] Pais-Correia AM, Sachse M, Guadagnini S, Robbiati V, Lasserre R, Gessain A, et al. Biofilm-like extracellular viral assemblies mediate HTLV-1 cell-to-cell transmission at virological synapses. Nat Med 2010;16:83–9.
[60] Colnot C, Ripoche MA, Milon G, Montagutelli X, Crocker PR, Poirier F. Maintenance of granulocyte numbers during acute peritonitis is defective in galectin-3-null mutant mice. Immunology 1998;94:290–6.
[61] Hsu DK, Yang RY, Pan Z, Yu L, Salomon DR, Fung-Leung WP, et al. Targeted disruption of the galectin-3 gene results in attenuated peritoneal inflammatory responses. Am J Pathol 2000;156:1073–83.
[62] de Boer RA, van der Velde AR, Mueller C, van Veldhuisen DJ, Anker SD, Peacock WF, et al. Galectin-3: a modifiable risk factor in heart failure. Cardiovasc Drugs Ther 2014;28:237–46.
[63] Garber K. Galecto biotech. Nat Biotechnol 2013;31:481.